JOURNAL OF GEOPHYSICAL RESEARCH, VOL. 108, NO. B3, 2134, doi:10.1029/2001JB000638, 2003

Reservoir depletion at The Geysers geothermal area, California, shown by four-dimensional seismic tomography

Rashmin C. Gunasekera[1]
Earthquake Hazards Team, U.S. Geological Survey, Menlo Park, California, USA

G. R. Foulger[2]
Department of Geological Sciences, University of Durham, Science Laboratories, Durham, UK

B. R. Julian
Earthquake Hazards Team, U.S. Geological Survey, Menlo Park, California, USA

Received 23 May 2001; revised 21 May 2002; accepted 25 June 2002; published 7 March 2003.

[1] Intensive geothermal exploitation at The Geysers geothermal area, California, induces myriads of small-magnitude earthquakes that are monitored by a dense, permanent, local seismometer network. Using this network, tomographic inversions were performed for the three-dimensional V_p and V_p/V_s structure of the reservoir for April 1991, February 1993, December 1994, October 1996, and August 1998. The extensive low-V_p/V_s anomaly that occupies the reservoir grew in strength from a maximum of 9% to a maximum of 13.4% during the 7-year study period. This is attributed to depletion of pore liquid water in the reservoir and replacement with steam. This decreases V_p by increasing compressibility, and increases V_s because of reduction in pore pressure and the drying of argillaceous minerals, e.g., illite, which increase the shear modulus. These effects serendipitously combine to lower V_p/V_s, resulting in a strong overall effect that provides a convenient tool for monitoring reservoir depletion. Variations in the V_p and V_s fields indicate that water depletion is the dominant process in the central part of the exploited reservoir, and pressure reduction and mineral drying in the northwest and southeast parts of the reservoir. The rate at which the V_p/V_s anomaly grew in strength in the period 1991–1998 suggests most of the original anomaly was caused by exploitation. Continuous monitoring of V_p, V_s, and V_p/V_s is an effective geothermal reservoir depletion monitoring tool and can potentially provide information about depletion in parts of the reservoir that have not been drilled. *INDEX TERMS:* 7280 Seismology: Volcano seismology (8419); 7230 Seismology: Seismicity and seismotectonics; 7205 Seismology: Continental crust (1242); 1645 Global Change: Solid Earth; *KEYWORDS:* geysers, tomography, four-dimensional, geothermal, reservoir, depletion

Citation: Gunasekera, R. C., G. R. Foulger, and B. R. Julian, Reservoir depletion at The Geysers geothermal area, California, shown by four-dimensional seismic tomography, *J. Geophys. Res.*, *108*(B3), 2134, doi:10.1029/2001JB000638, 2003.

1. Introduction

[2] The Geysers geothermal area in the northern Californian Coast Ranges is the largest exploited, vapor dominated geothermal reservoir in the world. It extends from approximately sea level, which is at about 1 km below the surface, down to at least 4.0 km below sea level (bsl) and has a surface area of ~75 km^2. Electricity generated at The Geysers comprises ~6% of northern California's electricity supply.

[3] The geology of The Geysers consists of mainly metamorphosed marine sedimentary and igneous rocks belonging to the Franciscan assemblage. The reservoir is bounded by the Collayomi fault zone to the northeast and the Mercuryville fault zone to the southwest (Figure 1). It is contained in fractured metagraywacke and an underlying felsite batholith. Felsite-hosted alteration and vein mineralization partially controlled by hydrothermal breccia increase permeability and fracture density within the steam reservoir [*Hulen and Nielson*, 1993]. The origin of the heat source at The Geysers is not well understood but it is postulated to be a magmatic intrusion or a body of partial melt in the midcrust [*Thompson*, 1992]. Teleseismic *P* wave arrival time delays and gravity data are consistent with such a body [*Iyer et al.*, 1981; *Blakely and Stanley*, 1993].

[4] Most of the heat is thought to be stored in the rock matrix and not in liquid pore water in the reservoir. Water

[1]Department of Geography, University of Cambridge, Cambridge, UK.
[2]Temporarily-at Volcano Hazards Team, U.S. Geological Survey, Menlo Park, California, USA.

0148-0227/03/2001JB000638$09.00

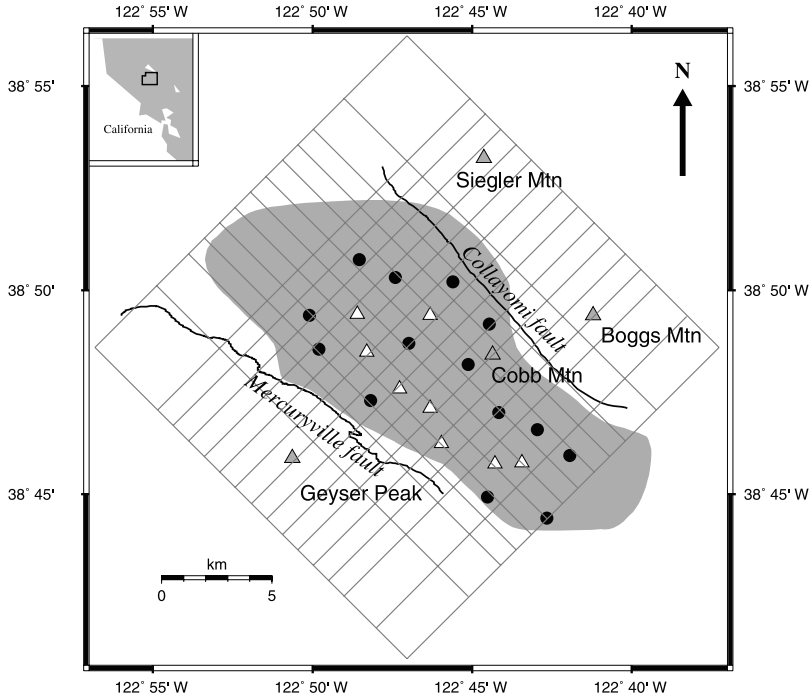

Figure 1. Map of The Geysers geothermal area. The production area is shaded. Solid circles, seismic stations with vertical sensors only; open triangles, three-component seismic stations, shaded triangles, geographic features as labeled. The grid shown was used for all the tomographic inversions and velocity nodes correspond to the intersections of the grid lines. The grid was rotated at 45° from north and centered on 38°48.60′N, 122°47.05′W. Inset shows the regional location of the main map.

flows out of the pores and flashes to steam in the boreholes during extraction. Significant commercial development at The Geysers began in 1960 with a 12 MW electrical power plant. Production increased at a rate of 63 MW per year until 1981. Between 1981 and 1989 power generation increased by 150 MW per year to peak at an unsustainable 1800 MW in 1987, when steam was extracted at a rate of $\sim 13.6 \times 10^6$ kg/h [*Barker et al.*, 1992].

[5] As a result of such a high rate of steam withdrawal, reservoir pressure declined steadily at an average rate of 11% per year. Pressure declined from 1987 by ~2.3 MPa to reach 1.2 MPa by the mid-1990s. Since then, methods such as reducing turbine inlet pressure, infill drilling, and water reinjection have been used to mitigate steam reservoir pressure decline. In 1995, due to a collapse in energy prices, economic curtailments were imposed resulting in very low production levels [*Barker and Pinogol*, 1997]. Thermal cycling damage to wells occurred during this period, wellhead pressure rose, and steam production declined further, especially during the winter months of 1995–1996 and 1996–1997 (A. Pinogol, personal communication, 2000). Water continued to be injected throughout this period, which reduced depletion. The normal reservoir temperature is ~240°C and this has remained fairly constant throughout the exploitation period.

[6] The seismic rate at The Geysers is as much as 45 times higher than that of the surrounding area, and over 140 M_L, 1.2 earthquakes occur per month. Most of this activity is thought to be induced by geothermal exploitation including both the removal of steam and fluid injection [*Eberhart-Phillips and Oppenheimer*, 1984; *Stark*, 1990; *Stark and Davies*, 1996]. Liquid reinjection may generate larger earthquakes than production [*Ross*, 1996]. Earthquakes have been strongly clustered in recent years, especially since 1995, and nondouble-couple source mechanisms have been identified that can potentially help to understand the earthquake genesis processes [*Ross*, 1996; *Ross et al.*, 1999].

[7] A field-wide permanent seismic network has been in place since 1989. For most of its operational period it was run by the UNOCAL Corporation. It is currently operated by Calpine. The network comprises 22 stations and covers the geothermal reservoir fairly uniformly. Eight stations have three-component sensors and the others only vertical sensors (Figure 1). Incoming data are digitized at 100 samples/s. The network changed little between 1991 and 1998, and is supplemented by permanent stations of the Northern California Seismic Network (NCSN) operated by the U.S. Geological Survey (USGS). An additional two small, dense networks have been operated intermittently in the northwest Geysers by the Central California Power Agency (CCPA) 1988–1989 and 1993–1994 [*Romero et al.*, 1994] and in the southeast Geysers by the Lawrence Berkeley Laboratories (LBL) 1992–1995 and 1997–1999 [*Kirkpatrick et al.*, 1997]. In addition, experiment-specific temporary networks have been operated at The Geysers from time to time.

[8] A 15-station, three-component digital network was operated by the U.S. Geological Survey during April 1991 [*Julian et al.*, 1996]. Using data collected with this network, combined with data from the 22-station UNOCAL network and local NCSN stations, high-quality V_p and V_p/V_s local earthquake tomography (LET) images of the geothermal

Table 1. Numbers of Data, Damping Values, Final RMS Residuals, Variance Reductions, Increase in the V_p/V_s Anomalies, and the Change in V_p/V_s Relative to the 1991 Epoch for the Four Post-1991 Inversions[a]

	Foulger et al. [1997] April 1991	This Study Feb. 1993	*Foulger et al.* [1997] Dec. 1994	This Study Oct. 1996	This Study Aug. 1998
Number of events	163	241	146	295	302
Number of data	2494	4043	3178	3762	4853
Number of *P* arrivals (Number of *P* picks per event)	2268 (14)	3444 (14)	2522 (17)	3193 (11)	4128 (14)
Number of *S* arrivals (Number of *S* picks per event)	226 (1.4)	599 (2.5)	656 (4.5)	569 (1.9)	725 (2.4)
V_p damp, s^2/km	5.0	20.0	5.0	5.0	5.0
V_p/V_s damp, s	2.0	20.0	2.0	5.0	2.0
Final RMS residual for arrivals, s	0.021	0.022	0.020	0.016	0.015
Final RMS residual for *S* arrivals, s	0.036	0.043	0.052	0.035	0.035
Variance reduction, %	75	9.3	13.9	15.5	26.3
Maximum amplitude of V_p/V_s anomaly at sea level	0.16	0.17	0.18	0.18	0.22
Change in V_p/V_s anomaly relative to 1991 at sea level, %	n/a	0.6	1.3	1.3	3.4

[a]Those inversions used the structure calculated for 1991 as a starting model; n/a, not available.

field were computed [*Julian et al.*, 1996]. The most significant finding was a strong V_p/V_s anomaly that correlates with the production zone. Theoretical considerations, laboratory experiments and field studies suggest that this low V_p/V_s anomaly represents a zone where the pore fluid is predominately vapor, pressure is low, and the shear modulus is increased as a result of the drying of argillaceous material in the reservoir rocks.[e.g., *Wang and Nur*, 1989; *Mavko and Mukerji*, 1995; *Boitnott and Boyd*, 1996; *Boitnott and Kirkpatrick*, 1997]. These changes probably resulted from the removal of reservoir fluids by production.

[9] *Ross* [1996] found that tomographic images of good quality could be obtained using only data from the 22-station permanent network operated then by the UNOCAL Corporation. This meant that four-dimensional LET might be used to study changes in reservoir structure with time. A repeat, field-wide V_p/V_s LET study of The Geysers was therefore performed using comparable data sets recorded in April 1991 and December 1994 on the UNOCAL network [*Foulger et al.*, 1997]. A significant increase in the strength of the low-V_p/V_s anomaly in the reservoir area during the 3-year interim period was detected. This was attributed to the effects of progressive fluid depletion of the reservoir. The current paper extends that work by conducting additional LET inversions using earthquakes recorded on the same network in February 1993, October 1996 and August 1998. The results show continuous depression of the V_p/V_s anomaly with time which we attribute to continued fluid depletion of the geothermal reservoir.

2. Method

[10] Data recorded on the UNOCAL network were obtained from the Northern California Earthquake Data Center. Well-recorded earthquakes providing uniform coverage of the reservoir were extracted for February 1993, October 1996, and August 1998 (Table 1). Good spatial coverage of the reservoir was achieved for all epochs (Figure 2). Few events were located in the northwest and southeast parts of the reservoir as these areas have relatively low seismic rates. Most events were shallower than 4.0 km bsl, which is the approximate base of the seismogenic layer.

[11] Arrival times were measured by hand using the interactive seismogram processing program epick. Where shear wave birefringence was noted the earliest *S* arrival was picked. *S* waves were picked only on horizontal components for all epochs. Only the highest-quality arrivals were selected, and the precision to which the onsets of the waves could be identified and picked is 0.01 s (one sample) for *P* waves and 0.02 s (two samples) for *S* waves. The program simulps12 [*Thurber*, 1983; *Evans et al.*, 1994] was used to invert the data. This program uses an iterative, damped least squares method to invert arrival times, simultaneously estimating earthquake locations and the three-dimensional V_p and V_p/V_s fields. The velocity structures are parametrized by values defined at the nodes of a three-dimensional grid, between which the V_p and V_p/V_s values are assumed to follow trilinear functions. We used nodes spaced at intervals of 1 km horizontally and vertically throughout most of the study volume (Figure 1). The grid extended from −2 km bsl (i.e., 2 km above sea level) down to 7 km bsl although only structure from about −1 km bsl to 2 km bsl is well resolved.

[12] *Julian et al.* [1996] and *Ross* [1996] obtained a tomographic model for The Geysers using a composite data set recorded in April 1991 on the UNOCAL and NCSN networks, and the temporary 15-station network deployed by the USGS. They followed a "graded inversion" approach. An initial inversion was conducted using a coarse nodal spacing of 10 km and a one-dimensional starting model obtained by first inverting the data using the program velest [*Kissling et al.*, 1994]. The resulting coarse three-dimensional model was interpolated to provide a starting model for an inversion with nodal spacing of 4.0 km. The nodal spacing was successively reduced to 2.0 and 1.0 km in the same manner. The final grid involved 1232 nodes. Damping values at each step were selected using damping trade-off curves that show the relationship between model complexity and data variance reduction for different damping values [*Evans and Achauer*, 1993]. A value of 1.74 was used as an a priori V_p/V_s ratio with the final 1-km grid.

[13] For our study, we inverted only the UNOCAL data from April 1991. We used the final 1991 model of *Julian et al.* [1996] and *Ross* [1996] as a starting model. The results for V_p, V_s, and V_p/V_s are shown in the left-hand panels of Figures 3a–3c, along with contours of the spread function, resolution, and standard error [*Toomey and Foulger*, 1989], which show the area of highest solution quality. All three parameters show that the central part of the reservoir is uniformly well imaged. Simulps12 inverts for V_p and V_p/V_s, and V_s is calculated from those results. Information regarding the errors in the V_s field is thus contained in the error fields for V_p and V_p/V_s, and therefore we do not plot error

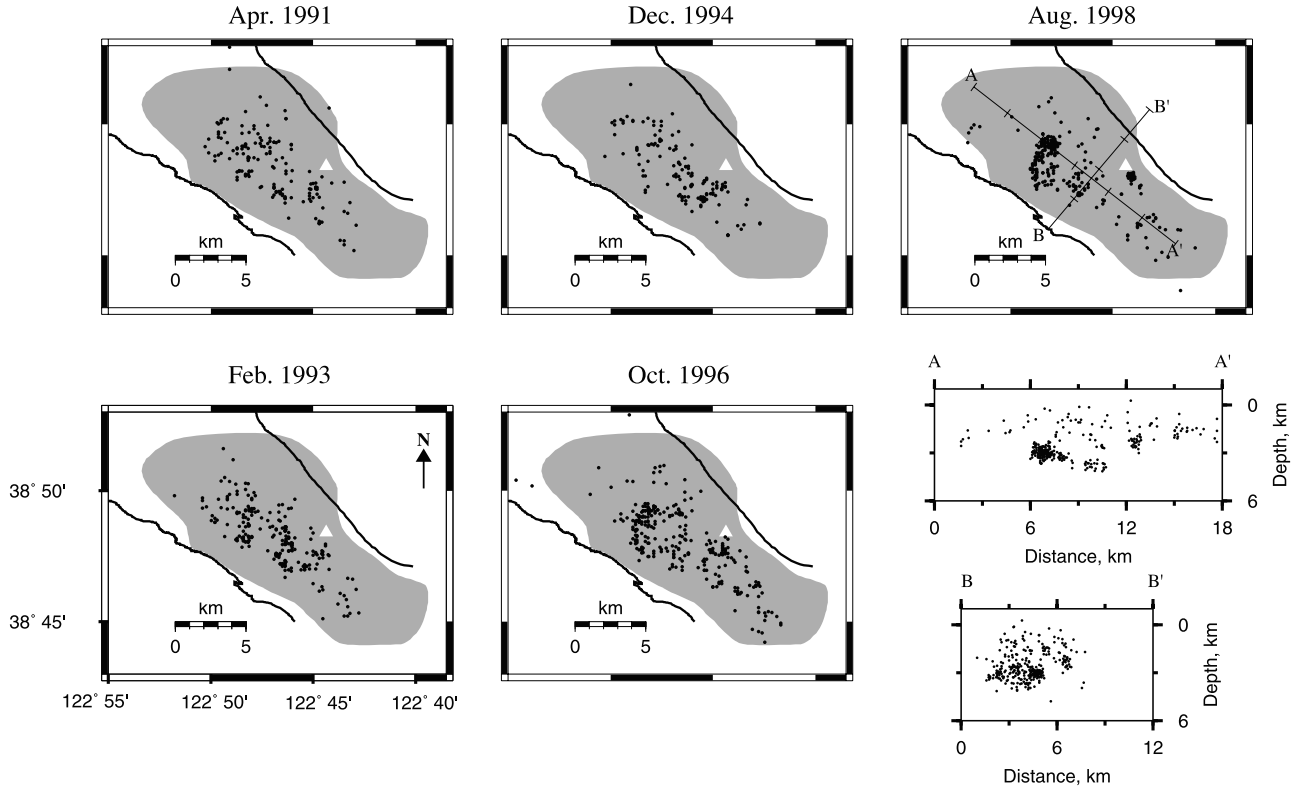

Figure 2. Maps showing the distribution of earthquakes used for the tomographic inversions for April 1991, February 1993, December 1994, October 1996, and August 1998. The earthquake epicenters after relocation through the final three-dimensional structures are shown as dots. Cross sections at bottom right are for August 1998 and show relocated earthquake hypocenters in NW-SE section (A–A′) and SW-NE section (B–B′). Open triangle corresponds to Cobb mountain. Thick solid lines show the Mercuryville fault in the southwest and the Colloyomi fault in the northeast.

contours for V_s (Figure 3b). Inversions of the subsequent epochs of data all used this model as the starting model and direct inversions were performed using nodes spaced at 1 km. The same nodal configurations were used for all inversions. The final RMS residual travel times are all in the range ~0.015–0.022 s for V_p and 0.035–0.052 for V_s (Table 1). Variance reductions were small for all inversions except April 1991 because the starting model used was very close to the final model. The variance reduction increased for later inversions, however, reflecting the fact that progressive structural change caused the starting model from 1991 to be increasingly further from the final model. The spread function, resolution, and standard error contours for subsequent years were all similar to those of the 1991 epoch and thus are not shown separately in the right-hand four panel pairs of Figures 3a and 3c.

3. Results

3.1. V_p, V_s, and V_p/V_s Anomalies in April 1991

[14] First-order spatial variations in the V_p and V_s structures at The Geysers determined from inversion of the April 1991 data are similar, and dominated by a substantial low wave speed volume in the northwest Geysers and higher wave speeds beneath the central and southeastern part (Figures 3a and 3b, left). These features probably reflect mostly variations in lithology since the effects of variations in the reservoir state are second-order effects [*Julian et al.*, 1996]. In the northwest Geysers at sea level and 1.0 km bsl low V_p and V_s anomalies characterize the caprock and normal reservoir that overlies the high-temperature reservoir. Velocities are higher in the central and southwest reservoir in rocks of the Franciscan assemblage.

[15] A strong, coherent low V_p/V_s anomaly correlates well with the steam reservoir (Figure 3c, left). It is wider to the northwest and southeast than in the middle, reflecting the general shape of the reservoir known from drilling. The anomaly does not extend beneath the extreme northwest and southeast parts of the reservoir. Station and earthquake coverage is good in the northwest Geysers, and if the anomaly extended beneath this area it would have been detected. To the southeast, however, station coverage is poor and few earthquakes occur, and the anomaly is imaged to the edge of the well-resolved volume. The anomaly might thus extend farther south, but this cannot be resolved with the current experiment. The strength of the low anomaly reaches 9% and was interpreted by *Julian et al.* [1996] to indicate a volume where much of the pore fluid was low-pressure vapor [*Barker et al.*, 1992; *Barker and Pinogol*, 1997], compared with the higher-pressure, liquid-dominated pore fluid in rocks outside the anomaly area.

3.2. Changes in the V_p, V_s, and V_p/V_s Anomalies Between April 1991 and August 1998

[16] Progressive, significant changes in the V_p, V_s, and V_p/V_s fields occur with time (Figures 3a–3c). In general, the

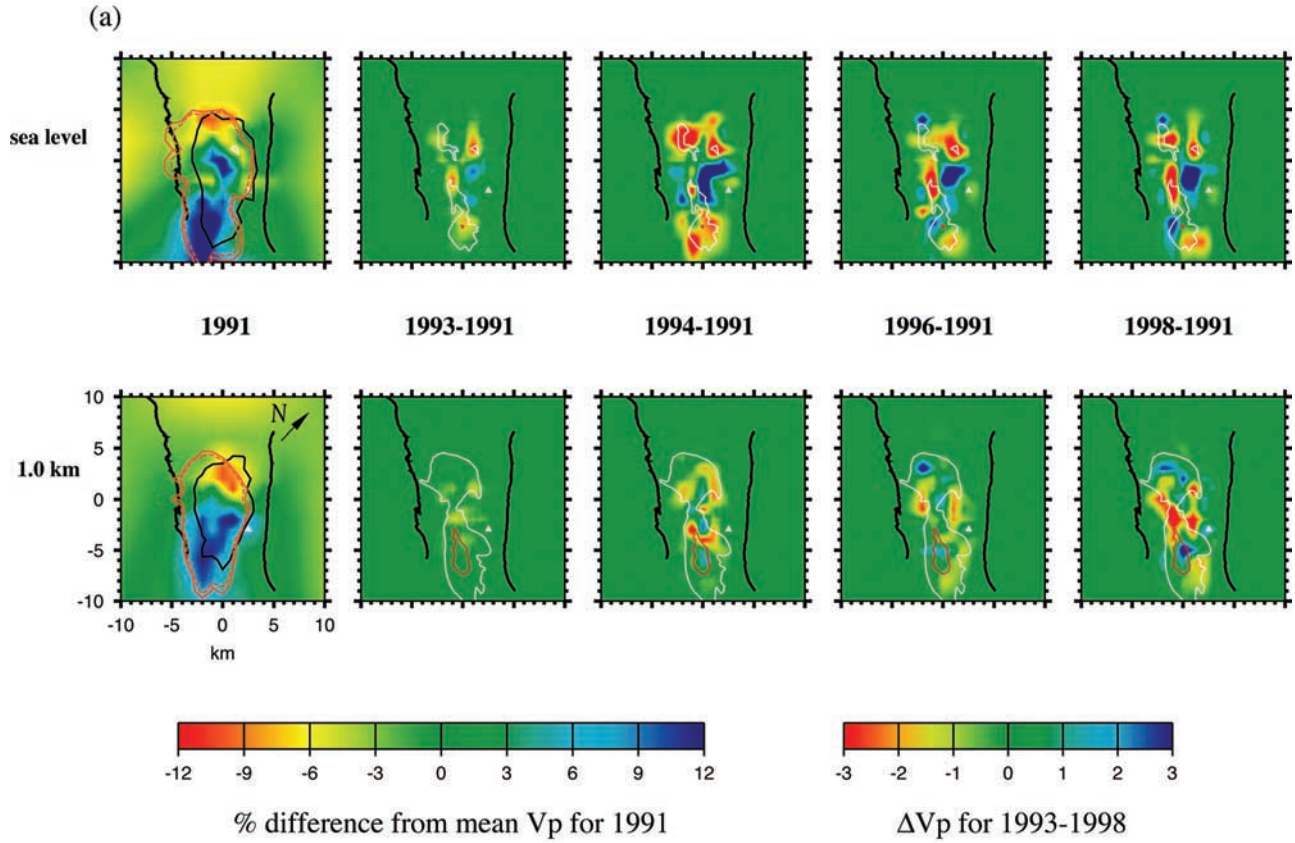

Figure 3. Anomalies in (a) V_p, (b) V_s, and (c) V_p/V_s at sea level (top) and 1.0 km bsl (bottom). Left pair of panels, which use the left color scale, show the structure for 1991. The black contour bounds the area within which the spread function is <2, the solid orange contour bounds the area within which the resolution is >0.01 (V_p) and >0.005 (V_p/V_s), and the dashed orange contour bounds the area within which the standard error is <0.0125 (V_p) and <0.005 (V_p/V_s). The three-dimensional model is most reliable within these contours. In peripheral regions, well outside the contours, the starting one-dimensional model is unperturbed. The remaining panels, which use the right color scale, show changes from the initial model for subsequent years. The white line encompasses the steam reservoir and the red boundary the felsite batholith that occupies the deeper parts of the reservoir. Spread, resolution, and standard error were similar for all epochs. The white triangle represents Cobb Mountain, and the thick black lines are the Mercuryville fault to the southwest and the Collayomi fault to the northeast. At the periphery of the areas shown, velocity is constrained only by the high-quality one-dimensional model calculated by simultaneous inversion [*Julian et al.*, 1996; *Ross*, 1996]. Velocities in this part of the area are displayed for comparison with those within the area well resolved by the LET inversions.

pattern of anomaly growth is smooth with time. The December 1994 epoch [*Foulger et al.*, 1997] is included for comparison purposes. Those data were picked by a different analyst, and the consistency of those results with the new epochs we study provides a useful indication of analyst-dependent variation in the results. In general, V_p and V_s decrease with time in the northwest and far southeast Geysers, and along the southern boundary of the reservoir. V_p and V_s increase at sea level beneath the northern boundary of the reservoir, but decrease at 1 km bsl beneath the same area. The patterns of change in V_p and V_s are broadly similar. Areas of coherent anomaly change trend northwest-southeast in general, parallel to the tectonic strike of the area. At sea level, V_p varies by −8.3% to +19.2% from the layer mean in 1991, but by 1998 these variations have increased to −10.2% to +23.6%. Changes in V_s are greater than those in V_p at both times. At sea level, V_s varies by −8.4% to 29.3% in 1991 but by 1998 this has increased to −10.4 to 41.4%. At 1.0 km bsl changes in V_p and V_s with time are less than at sea level.

[17] The strength of the V_p/V_s anomaly progressively increased between 1991 and 1998 (Figure 3c). As is the case for the V_p and V_s fields, the December 1994 epoch is consistent with the other epochs in the sense of the anomaly, but deviates from the trend regarding amplitude, reflecting analyst-dependent variations. At sea level, by 1993 two distinct areas of V_p/V_s anomaly growth had developed with increases in anomaly strength of up to 0.6%. Both anomalies increased progressively in strength and size with time and by August 1998 a third negative V_p/V_s anomaly had developed farther north. The increase in anomaly strength by 1998 was up to a maximum of 3.4%.

[18] At 1 km bsl, in February 1993 a single area of anomaly growth is detected in the center of the reservoir.

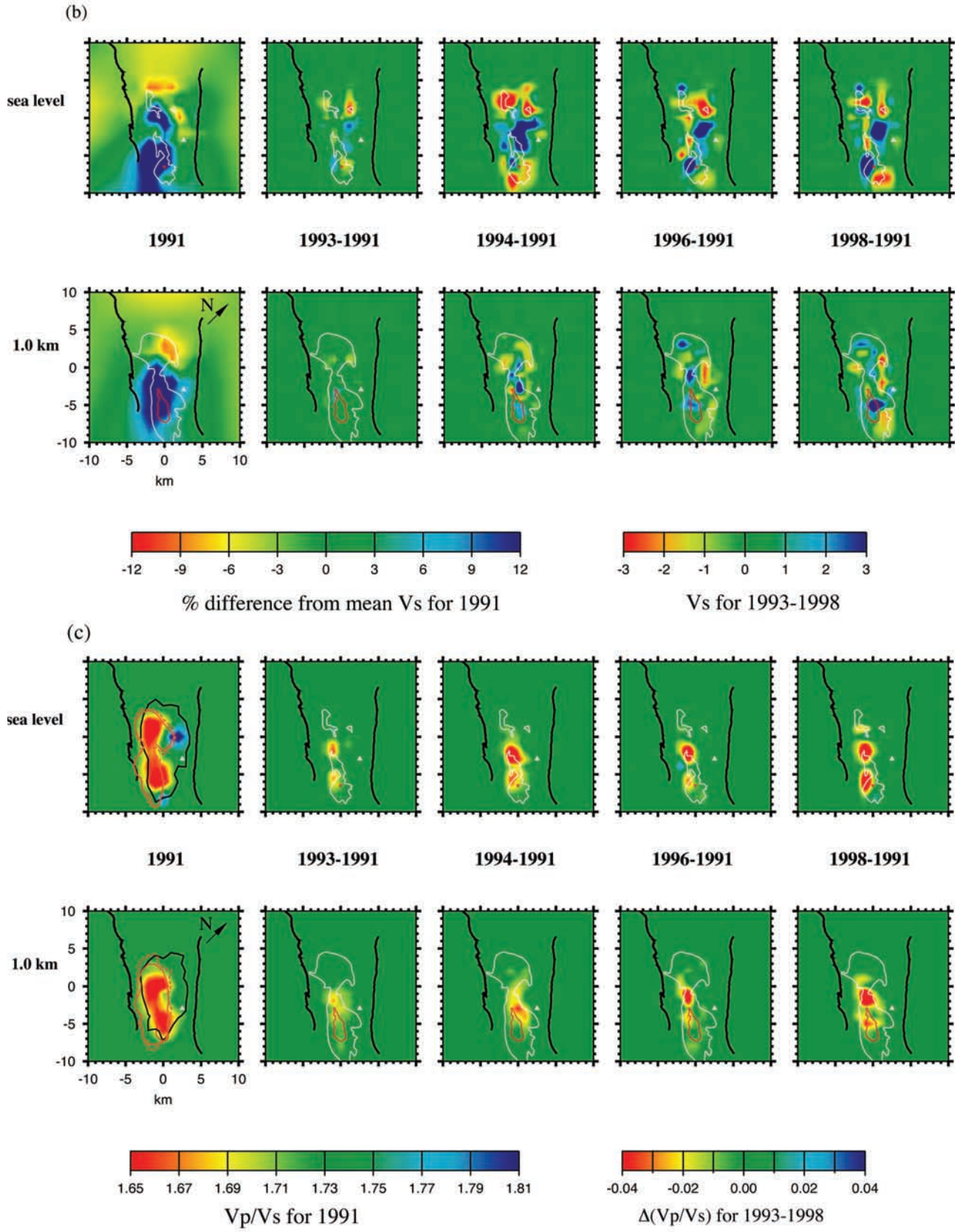

Figure 3. (continued)

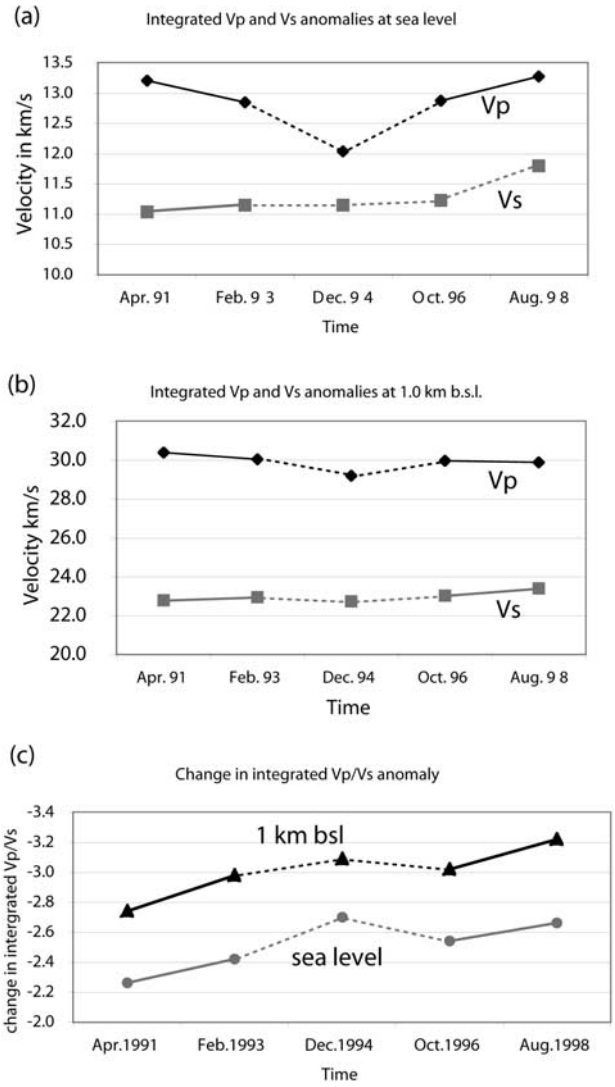

Figure 4. Plots of integrated anomalies in V_p, V_s, and V_p/V_s at sea level and 1.0 km bsl as a function of time. The deviation of the 1994 epoch from the general trend indicates the degree of analyst-dependent variation to be expected. (a) Change in integrated anomaly for V_p and V_s at sea level, (b) same as Figure 4a but for 1.0 km bsl, and (c) the change in integrated (negative) V_p/V_s anomaly with time at sea level and 1.0 km bsl.

This increased in strength by October 1996 and a second area of anomaly growth developed farther to the south. By 1998, these two areas of growth had increased further in strength, were up to 4.8% stronger than in 1991, and a third area of anomaly growth existed to the north.

[19] At 2 km bsl a single area of anomaly growth was detected directly below the strongest, central area of anomaly growth at 1 km bsl This anomaly increased in strength by up to 4.6% between April 1991 and August 1998.

3.3. Development in Integrated V_p, V_s, and V_p/V_s Anomalies

[20] The variations in V_p, V_s, and V_p/V_s with time at sea level and 1 km bsl are shown in Figure 4 as variations in the spatially integrated anomalies. These are, for each parameter, the arithmetic sum of the deviations from the average starting value for each depth. The total V_p anomaly at both sea level (Figure 4a) and 1 km bsl (Figure 4b) is not significantly different in 1998 from its 1991 value. As mentioned above, the December 1994 epoch is less consistent with the general trend than the other epochs. The lower values for the integrated V_p anomaly for the February 1993 and October 1996 epochs are consistent with the very low December 1994 value, but given the errors in our results (see section 4) this trend is unlikely to be significant. The integrated V_s, and V_p/V_s anomalies increased monotonically between April 1991 and August 1998. As for V_p, the December 1994 epoch deviates somewhat from the trend of the other three post-1991 epochs in V_p/V_s.

[21] The relationships of V_p/V_s to V_p and V_s, along with regression lines, are shown in Figure 5a. All velocity nodes that changed between April 1991 and August 1998 at sea level and 1 km bsl are plotted. At both sea level and 1 km bsl, V_p/V_s is weakly anticorrelated with V_p but strongly anticorrelated with V_s. No statistically significant correlation between V_p/V_s and V_p was established. In the case of V_s, a significant negative correlation with V_p/V_s was detected with a slope of -0.47 ± 0.06 at sea level and -0.33 ± 0.04 at 1.0 km bsl

[22] The results of *Romero et al.* [1995] for the northwest Geysers (Figure 5b) and *Kirkpatrick et al.* [1997] for the southeast Geysers (Figure 5c) and the results of a stochastic model simulation [*Boitnott*, 1995] (Figure 5d) show a similar result, with variations in V_p/V_s apparently being caused in general by variations in V_s. Anomalously low values of V_p/V_s apparently result, in general, from anomalously high values of V_s.

4. Discussion

[23] The V_p/V_s anomaly in the steam reservoir volume increased in strength fairly regularly over the 7-year period studied, which is in itself compelling evidence that the progression is real and not an artefact of errors. It is nonetheless important to appreciate potential sources of bias in the results. The size of the data sets and distribution of events varied between epochs (Table 1 and Figure 2). The effect of this was investigated by splitting the 1993 data set into two halves, each containing ~120 events, and inverting each half separately. The differences in the final V_p/V_s structures were smaller than 0.015 [*Gunasekera*, 2001]. This suggests that for this experimental setup, little is gained by using more than ~120 earthquakes. The picking of arrival times, in particular of *S* wave arrival times is highly analyst-dependent. The effect of this was explored by comparing our results with those from an inversion of data from December 1994 (Figures 3 and 4) [*Foulger et al.*, 1997]. The December 1994 data set involved significantly more picks per event. In particular, the number of *S* wave picks per event (4.5) was over twice what we picked for the other inversions (1.4–2.5), and the final RMS residual for *S* arrivals was exceptionally large. This suggests that the overall quality of picks included in that inversion was poorer. We further investigated the December 1994 epoch by repicking and relocating a subset of events [*Gunasekera*, 2001]. The results suggested that the events may have been picked systemati-

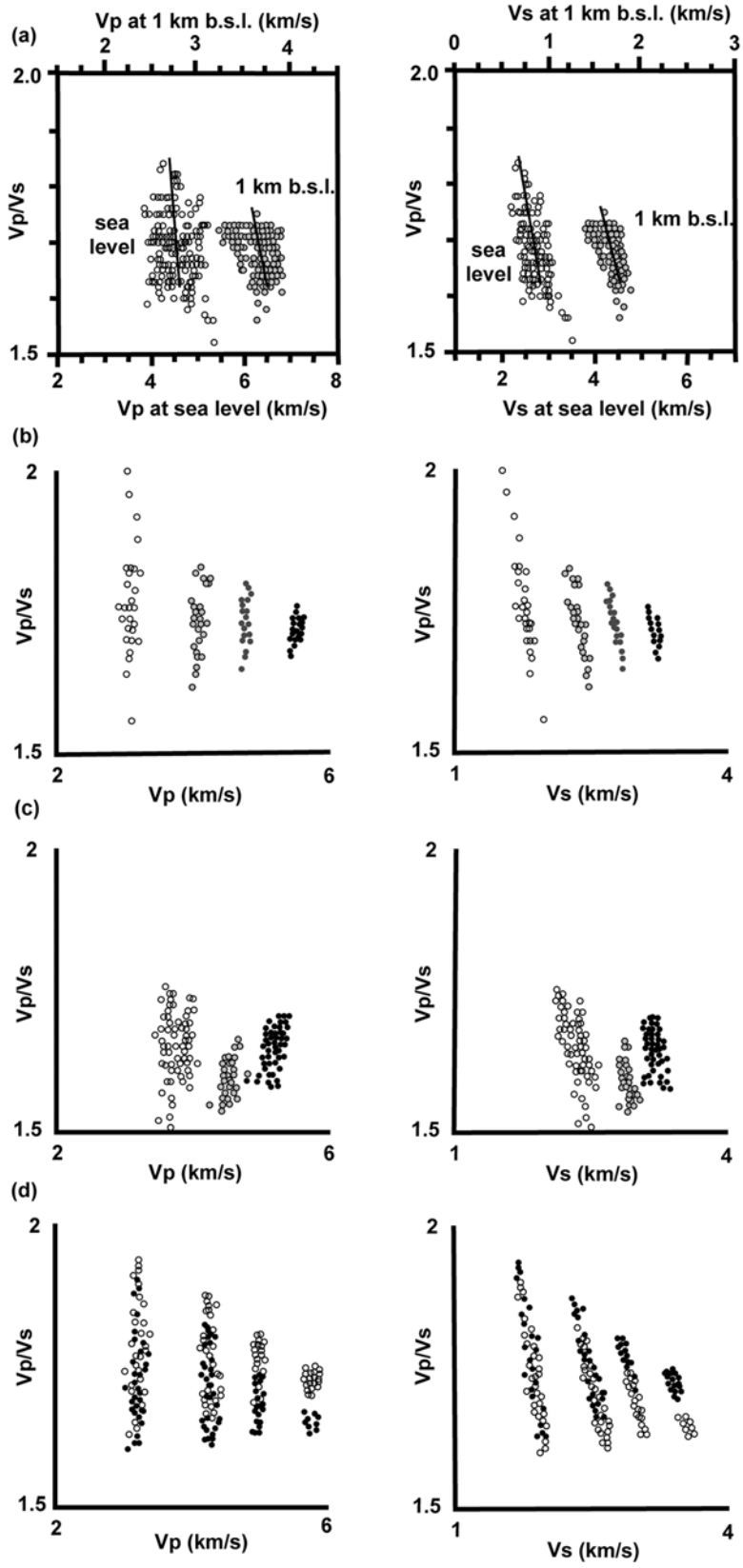

Figure 5. The relationship between V_p/V_s, V_p, and V_s. (a) Results from this study. Shaded dots indicate data from sea level, and solid dots indicate data from 1 km bsl. Regression lines calculated are shown (see text for details). (b) Results of *Romero et al.* [1995] for the northwest Geysers. Different symbols correspond to different depths. (c) Results of *Kirkpatrick et al.* [1997] for the southeast Geysers. Different symbols correspond to different depths. (d) Results from a stochastic model simulation [*Boitnott and Kirkpatrick*, 1997]. Open symbols represent a dry matrix, and solid symbols represent a wet matrix.

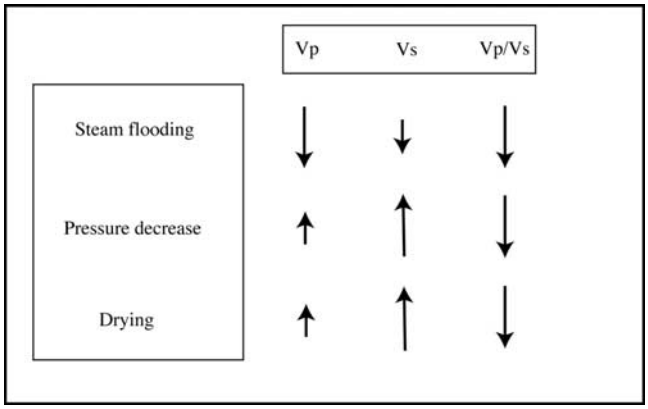

Figure 6. Schematic illustrating the effects of processes caused by exploitation at The Geysers on V_p, V_s, and V_p/V_s. Large arrows indicate the dominant effect, and small arrows indicate subsidiary or negligible effects. The three processes have differing effects on V_p and V_s, but all cause V_p/V_s to decrease.

cally later, and located systematically deeper, than was the case for the other epochs. This may account for the apparently spurious decrease in V_p in general for the December 1994 epoch, which causes the very strong apparent decrease in V_p/V_s for that epoch. A relatively small number of events were used for the April 1991 epoch, but the numbers of P and S picks per event were similar to those for the February 1993, October 1996, and August 1998 epochs, suggesting that the picks were of a similar quality.

[24] The earthquakes used for the August 1998 inversion are significantly more clustered than other epochs. We investigated the effect of this by removing most of the clustered events and comparing the V_p/V_s inversion results with those obtained using the entire data set. There were only very small differences in the two results. The final RMS residuals for P and S wave arrival times (Table 1) indicate the part of the residuals that could not be explained by three-dimensional structure. These are typically 0.02 s for P waves and 0.04 s for S waves. These are approximately twice the estimated picking precisions of 0.01 s and 0.02 s and result from sources of error such as misidentification of arrivals and unmodeled effects, e.g., variable anisotropy and small-scale structure.

[25] We also investigated the effect of using a different base starting model. We used the model obtained by *Julian et al.* [1996] for 1991 using a combination of the UNOCAL and NCSN networks, augmented with 15 additional temporary three-component stations operated for one month in 1991 by the U.S. Geological Survey. We inverted the 1998 data set using this model as a starting model, and differenced the results with the 1991 model of *Julian et al.* [1996]. The growth in the V_p/V_s anomaly determined using that base model was very similar in spatial pattern to that obtained using the 1991 base model determined using the UNOCAL network only. The maximum strength of the anomaly growth between 1991 and 1996, however, was 4.6% when the three-network base model was used, compared with 3.4% when the one-network base model was used. This suggests that the results presented here, and shown in Figure 3, are robust estimates of the pattern, and conservative estimates of the strength of anomaly growth.

[26] Factors that affect V_p, V_s, and V_p/V_s at The Geysers include lithology, temperature, pore pressure and pore fluid phase. Of these, the temperature of the reservoir has remained fairly constant in recent years (M. Stark, personal communication, 2000), despite exploitation. Thus changes in pore pressure, pore fluid phase, and the water content of minerals caused by steam removal are probably responsible for the changes observed in the anomaly, and the effects of these factors on V_p, V_s, and V_p/V_s are shown schematically in Figure 6.

[27] The effect of replacing liquid pore fluid with vapor has been quantitatively studied in the McElroy oil field, west Texas. The McElroy oil field is a good analog of The Geysers. Porosity and permeability are variable, with an average porosity of 10% and permeabilities in the range $0.01-90 \times 10^{-11}$ cm^2. The reservoir rock comprises dolostones and evaporite cement and was flooded with CO_2 at a depth of 900 m below the surface in order to improve oil recovery. At the time of CO_2 flooding the pore fluid was half water and half oil. The effect of flooding was monitored seismically. V_p was found to be reduced by 2–4% on average by CO_2 flooding, and up to 9% in areas of high porosity, while V_s was little affected [*Wang et al.*, 1998]. However, associated local increases in pore pressure accompanying the CO_2 flooding reduced V_s as a result of reduction in the shear modulus. In the case of the McElroy field, reduction in V_p and V_s went hand in hand and the net result was little change in V_p/V_s [*Wang and Nur*, 1989].

[28] Similar behavior has also been observed in laboratory experiments with reservoir rock samples, where an increase in pore pressure from 8.3 to 15.9 MPa at constant overburden pressure of 20 MPa caused V_p to decrease by 1.7% and V_s by 2.6% [*Wang et al.*, 1998]. An increase in V_s with decreasing pore pressure was also observed in water-filled Berea sandstone at constant temperature of 145° C and other conditions representative of a steam reservoir. In that experiment, V_p/V_s was observed to decrease from 1.78 to 1.67 as pore pressure decreased by 0.3 MPa and water converted to steam [*Ito et al.*, 1979]. At The Geysers, the removal of steam has the effect of causing pore water to be replaced by vapor, accompanied by a pressure decrease [e.g., *Lipman et al.*, 1978]. Reservoir pressure data are proprietary, but pressure is known to have decreased from ~3.5 to ~0.8 MPa by the mid-1990s [*Barker and Pinogol*, 1997]. These two processes have the effect of decreasing V_p and increasing V_s, both of which will lower V_p/V_s [e.g., *Boitnott*, 1995]. This situation contrasts with that of the McElroy field where CO_2 flooding is accompanied by a pressure *increase* and the effects on V_p/V_s tend to cancel out [e.g., *Wang and Nur*, 1989].

[29] A third effect may decrease V_p/V_s still further. Water saturation has an unusually large chemical-mechanical weakening effect on argillaceous minerals such as illite, which are abundant at The Geysers. This has been explained using modified Biot poroelastic theory [*Boitnott*, 1995; *Boitnott and Kirkpatrick*, 1997]. As pore fluid is removed and the minerals dry, and V_p/V_s is lowered because V_s increases (the "spaghetti effect" [*Rombauer and Becker*, 1975, pp. 212–213]). Thus, three different processes at The

Geysers related to fluid saturation serendipitously reinforce one another to decrease V_p/V_s (Figure 6).

[30] The effect of saturation is depth-dependent [*Boitnott and Kirkpatrick*, 1997]. At moderate depths within the reservoir V_p/V_s is largely controlled by the rock matrix properties, with a higher V_p/V_s for a saturated matrix than a dry matrix [*Boitnott and Kirkpatrick*, 1997]. At shallower depths, the effect of saturation on the rock matrix is diminished by the effect of field-scale compliant features such as joints and faults [*Boitnott and Kirkpatrick*, 1997]. The clear anticorrelation of V_s and V_p/V_s and the lack of a significant correlation between V_p and V_p/V_s (Figure 5) suggest that the effects of pressure decrease and mineral drying are predominant at The Geysers.

[31] While the progressive growth in V_p/V_s ultimately results from depletion of liquid water in the reservoir, comparison of the separate V_p and V_s fields (Figures 5a and 5b) suggests that different effects may be dominant in different parts of the field. At sea level, the most southeasterly and the most northwesterly areas of V_p/V_s anomaly growth (Figure 3c, top right) correlate with areas of progressive increase in V_s of up to 0.05 km/s from 1991 to 1998. This is also the case for the deeper continuation of the southeasterly anomaly at 1 km bsl This suggests that the strongest effects in this area are pressure decrease and mineral drying. In contrast, the middle anomaly at sea level and its continuation down to 1 km bsl are predominately caused by decrease in V_p of up to 0.27 km/s from 1991 to 1998, suggesting that reduction in compressibility due to the replacement of pore water by steam is the predominant effect. This is in agreement with the known higher liquid content of the central Geysers compared with the northwest Geysers.

[32] Variation in the dominant mechanism causing seismic wave speed evolution at The Geysers may be partly related to the pattern of water reinjection. This is being progressively increased in an effort to slow reservoir decline. It increased from 33% to 58% of the fluid extracted between 1994 and 1996 [*Barker and Pinogol*, 1997]. Most of this brine, however, is reinjected in the extreme southeast of the reservoir, outside our resolvable area, and the amounts of reinjectate and the locations of the injector wells are proprietary. It is thus not possible currently to assess quantitatively the effect of reinjection.

[33] The low-V_p/V_s anomaly observed at The Geysers correlates with the volume where the pore fluid is thought to be vapor-dominated, where pore pressure is relatively low and argillaceous minerals relatively dry [e.g., *McLaughlin*, 1981]. *Julian et al.* [1996] concluded that The Geysers might have had an associated low-V_p/V_s anomaly prior to development, since such conditions probably existed naturally then. Between April 1991 and August 1998 the anomaly grew in strength by up to $\sim$0.5%/yr at 1 km bsl At this rate, the anomaly observed in 1991, which had a maximum strength of $\sim$9%, would have taken $\sim$18 years to develop. Rates of steam extraction are presented by *Barker et al.* [1992]. During the period 1991–1998, the rate of steam extraction was $\sim 7-9 \times 10^{10}$ kg/yr. Prior to this, it increased from low levels in the 1960s to peak at $\sim 11 \times 10^{10}$ kg/yr in 1987, and decreased subsequently. Over the 32-year period 1960–1991, the average rate of steam production was $\sim 5 \times 10^{10}$ kg/yr, or equivalent to 18–23 years of production at $7-9 \times 10^{10}$ kg/yr. This suggests that the total production at The Geysers could account for the whole of the V_p/V_s anomaly. On the other hand, low-V_p/V_s anomalies have been reported for unexploited geothermal areas. For example, *Foulger et al.* [1995] and *Miller et al.* [1998] report V_p/V_s anomalies as strong as -4% in the area of most abundant hot springs and fumaroles in the unexploited Grensdalur geothermal field, Iceland. Thus, although exploitation at The Geysers could conceivably account for all of the observed V_p/V_s anomaly, it is possible that an anomaly existed there originally. The association of low-V_p/V_s anomalies and geothermal reservoirs might be important to the study of new prospects.

[34] Repeated LET has also been used to investigate the migration of pore fluid at Mammoth Mountain, an active volcanic cone in Long Valley caldera, California [*Foulger et al.*, 2003]. Mammoth Mountain has been degassing up to 2×10^8 kg/yr of CO_2 since 1989. Significant changes in the V_p, V_s, and V_p/V_s fields were detected that are consistent with the migration of CO_2 into the center of the volcanic edifice. There, pressure increased, while in peripheral areas pressure decreased. In contrast to the situation at The Geysers, the effects of CO_2 flooding and pressure changes at Mammoth Mountain on V_p/V_s partially cancelled out, and changes in the V_p/V_s field were less diagnostic of fluid migration. The reinforcement of changes in the V_p/V_s anomaly by the various reservoir effects at The Geysers, and perhaps other geothermal fields, renders V_p/V_s a serendipitously useful parameter for monitoring geothermal reservoir evolution.

5. Conclusions

[35] Commercial exploitation of The Geysers geothermal area is causing changes in local seismic structure that are detectable using repeated LET at 2-year intervals. The progressive depletion of pore fluid causes the replacement of pore liquid with vapor. This increases compressibility, thereby reducing V_p, and also causes pore pressure decrease and the drying of argillaceous minerals such as illite. Both of these processes increase the shear modulus and V_s. These three effects reinforce one another in reducing V_p/V_s.

[36] In the period April 1991 to August 1998, three areas in the reservoir exhibited reductions in V_p/V_s of up to 4.6% consistent with these effects. Examination of the separate V_p and V_s fields indicates that water depletion was the most important process in the central part of the exploited reservoir, with pressure reduction and mineral drying being stronger effects in the northwest and southeast parts of the reservoir.

[37] The rate at which the V_p/V_s anomaly grew in strength between April 1991 and August 1998 suggests that the entire anomaly might have been caused by industrial activity since the early 1960s. However, the observation that unexploited geothermal fields also exhibit low-V_p/V_s anomalies suggests that only part of the low-V_p/V_s anomaly may have been caused by exploitation.

[38] The degree to which these results can be calibrated quantitatively is limited because much of the well data at The Geysers, including the quantities of fluid extracted and reinjected, are proprietary. Continuous monitoring of the three-dimensional V_p, V_s, and V_p/V_s fields is an effective

method of monitoring reservoir depletion at The Geysers, and probably also at other seismically active exploited geothermal areas. This technique may, in particular, provide information about depletion in parts of the reservoir that are being tapped indirectly but have not been drilled.

[39] **Acknowledgments.** We thank Doug Neuhauser, at Northern California Earthquake Data Center (NCEDC), for providing UNOCAL raw seismogram data used in this study, the UNOCAL Corporation for providing seismic data, and Phil Dawson, Ruth Harris, John Evans, Jake Lowenstern, and an anonymous reviewer for helpful reviews. Figures were prepared using the Generic Mapping Tools (GMT) software [*Wessel and Smith*, 1991].

References

Barker, B. J., and A. S. Pinogol, Geysers reservoir performance—An update, paper presented at 22nd Workshop on Reservoir Engineering, Stanford Univ., Stanford, Calif., 1997.

Barker, B. J., M. S. Gulati, M. A. Bryan, and K. L. Riedel, Geysers reservoir performance, in *Monograph on The Geysers Geothermal Field*, edited by C. Stone, *Spec. Rep. 17*, pp. 167–177, Geotherm. Resour. Counc., Davis, Calif., 1992.

Blakely, R. J., and W. D. Stanley, The Geysers magma chamber, California: Constraints from gravity data, density measurements and well information, *Trans. Geotherm. Resour. Counc.*, *17*, 227–233, 1993.

Boitnott, G. N., Laboratory measurements on reservoir rocks from The Geysers geothermal field, paper presented at Twentieth Workshop on Geothermal Reservoir Engineering, Stanford Univ., Stanford, Calif., 1995.

Boitnott, G. N., and P. J. Boyd, Permeability, electrical impedance, and acoustic velocities on reservoir rocks from The Geysers geothermal field, paper presented at Twenty-first Workshop on Geothermal Reservoir Engineering, Stanford Univ., Stanford, Calif., 1996.

Boitnott, G. N., and A. Kirkpatrick, Interpretation of field seismic tomography at The Geysers geothermal field, California, paper presented at Twenty-second Workshop on Geothermal Reservoir Engineering, Stanford Univ., Stanford, Calif., 1997.

Eberhart-Phillips, D., and D. H. Oppenheimer, Induced seismicity in the Geysers geothermal area, California, *J. Geophys. Res.*, *89*, 1191–1207, 1984.

Evans, J. R., and U. Achauer, Teleseismic velocity tomography using the ACH method: Theory and application to continental-scale studies, in *Seismic Tomography: Theory and Applications*, edited by H. M. Iyer and K. Hirahara, pp. 319–360, Chapman and Hall, New York, 1993.

Evans, J. R., D. Eberhart-Phillips, and C. H. Thurber, User's manual for SIMULPS12 for imaging V_P and V_P/V_S, a derivative of the Thurber tomographic inversion SIMUL3 for local earthquakes and explosions, *U.S. Geol. Surv. Open File Rep., 94-431*, 142 pp., 1994.

Foulger, G. R., A. D. Miller, B. R. Julian, and J. R. Evans, Three-dimensional V_p and V_p/V_s structure of the Hengill triple junction and geothermal area, Iceland, and the repeatability of tomographic inversion, *Geophys. Res. Lett.*, *22*, 1309–1312, 1995.

Foulger, G. R., C. C. Grant, A. Ross, and B. R. Julian, Industrially induced changes in Earth structure at The Geysers geothermal area, California, *Geophys. Res. Lett.*, *24*, 135–137, 1997.

Foulger, G. R., B. R. Julian, A. M. Pitt, D. P. Hill, P. Malin, and E. Shalev, Three-dimensional crustal structure of Long Valley caldera, California, and evidence for the migration of CO2 under Mammoth Mountain, *J. Geophys. Res.*, *108*, doi:10.1029/2000JB000041, in press, 2003.

Gunasekera, R. C., Induced seismicity and environmental change at The Geysers geothermal area, California, Ph.D. thesis, Univ. of Durham, Durham, U. K., 2001.

Hulen, J. B., and D. L. Nielson, Interim report on geology of The Geysers felsite, northwestern California, *Trans. Geoterm. Resour. Counc.*, *17*, 249–258, 1993.

Ito, H., J. De Vilbiss, and A. Nur, Compressional and shear waves in saturated rock during water-steam transition, *J. Geophys. Res.*, *84*, 4731–4735, 1979.

Iyer, H. M., D. H. Oppenheimer, T. Hitchcock, J. N. Roloff, and J. M. Coakley, Large teleseismic P-wave delays in The Geysers-Clear Lake geothermal area, in *Research in The Geysers-Clear Lake Geothermal Area, Northern California*, edited by R. J. McLaughlin and J. M. Donnelly-Nolan, *U.S. Geol. Surv. Prof. Pap.*, *1141*, 97–116, 1981.

Julian, B. R., A. Ross, G. R. Foulger, and J. R. Evans, Three-dimensional seismic image of a geothermal reservoir: The Geysers, California, *Geophys. Res. Lett.*, *23*, 685–688, 1996.

Kirkpatrick, A., J. E. Peterson, and E. L. Majer, Three-dimensional compressional and shear wave seismic velocity models for the southeast Geysers, paper presented at Twenty-second Workshop on Reservoir Engineering, Stanford Univ., Stanford, Calif., 1997.

Kissling, E., W. L. Ellsworth, D. Eberhart-Phillips, and U. Kradolfer, Initial reference models in local earthquake tomography, *J. Geophys. Res.*, *99*, 19,635–19,646, 1994.

Lipman, S. C., C. J. Strobel, and M. S. Gulati, Reservoir performance of The Geysers, *Geothermics*, *7*, 209–291, 1978.

Mavko, G., and T. Mukerji, Seismic pore space compressibiliby and Gassman's relation, *Geophysics*, *60*, 1743–1749, 1995.

McLaughlin, R. J., Tectonic setting of pre-Tertiary rocks and its relation to geothermal resources in The Geysers-Clear Lake area, in *Research in The Geysers-Clear Lake Geothermal Area, Northern California*, edited by R. J. McLaughlin and J. M. Donnelly-Nolan, *U.S. Geol. Surv. Prof. Pap.*, *1141*, 3–24, 1981.

Miller, A. D., B. R. Julian, and G. R. Foulger, Three-dimensional seismic structure and moment tensors of non-double-couple earthquakes at the Hengill-Grensdalur volcanic complex, Iceland, *Geophys. J. Int.*, *133*, 309–325, 1998.

Rombauer, I. S., and M. R. Becker, *Joy of Cooking*, 915 pp., Bobbs-Merrill, Indianapolis, Indiana, 1975.

Romero, A. E., A. Kirkpatrick, E. L. Majer, and J. E. Peterson, Seismic monitoring at The Geysers geothermal field, *Trans. Geotherm. Resour. Counc.*, *18*, 331–338, 1994.

Romero, A. E., T. V. McEvilly, E. L. Majer, and D. Vasco, Characterisation of the geothermal system beneath the northwest Geysers steam field, California, from seismicity and velocity patterns, *Geothermics*, *24*, 471–487, 1995.

Ross, A., The Geysers geothermal area, California: Tomographic images of the depleted steam reservoir and non-double-couple earthquakes, Ph.D. thesis, Univ. of Durham, Durham, U. K., 1996.

Ross, A., G. R. Foulger, and B. R. Julian, Source processes of industrially-induced earthquakes at The Geysers geothermal area, California, *Geophysics*, *64*, 1877–1889, 1999.

Stark, M. A., Imaging injected water in The Geysers reservoir using microearthquake data, *Trans. Geotherm. Resour. Counc.*, *17*, 1697–1704, 1990.

Stark, M. A., and S. D. Davies, Remotely triggered microearthquakes at The Geysers geothermal field, California, *Geophys. Res. Lett.*, *23*, 945–948, 1996.

Thompson, R. C., Structural stratigraphy and intrusive rocks at The Geysers geothermal field, in *Monograph on The Geysers Geothermal Field*, edited by C. Stone, pp. 59–63, *Geotherm. Resour. Counc.*, Davis, Calif., 1992.

Thurber, C. H., Earthquake locations and three-dimensional crustal structure in the Coyote Lake area, central California, *J. Geophys. Res.*, *88*, 8226–8236, 1983.

Toomey, D. R., and G. R. Foulger, Tomographic inversion of local earthquake data from the Hengill-Grensdalur central volcano complex, Iceland, *J. Geophys. Res.*, *94*, 17,497–17,510, 1989.

Wang, Z., and A. M. Nur, Effects of CO_2 flooding on wave velocities in rocks with hydrocarbons, *Soc. Pet. Eng. Res. Eng.*, *3*, 429–436, 1989.

Wang, Z., M. E. Cates, and R. T. Langen, Seismic monitoring of CO_2 flooding of a carbonate reservoir: A rock physics study, *Geophysics*, *63*, 1604–1617, 1998.

Wessel, P., and W. H. F. Smith, Free software helps map and display data, *Eos Trans. AGU*, *72*, 445–446, 1991.

R. C. Gunasekera, Department of Geography, University of Cambridge, Cambridge, UK. (Rashmin@dunelm.org.uk)

G. R. Foulger and B. R. Julian, Earthquake Hazards Team, U.S. Geological Survey, 345 Middlefield Rd., MS 977, Menlo Park, CA 94025, USA. (foulger@swave.wr.usgs.gov; julian@usgs.gov)